

Simplification of tensor updates toward performance-complexity balanced quantum computer simulation

Koichi Yanagisawa, Aruto Hosaka, and Tsuyoshi Yoshida

Information Technology R&D Center, Mitsubishi Electric Corporation, Kanagawa 247-8501, Japan

(Dated: June 6, 2024)

Tensor network methods have evolved from solving optimization problems in quantum many-body spin systems. While the tensor network is now regarded as a powerful tool in quantum computer simulation, there still exists a complexity issue in updating the tensors. This work studies the tensor updates simplification in the context of the tensor network based quantum computer simulation. According to the numerical simulations, a method called simple update, also originated in quantum many-body spin systems, shows a good balance of the fidelity and the computational complexity.

I. INTRODUCTION

Quantum computing research is now entering the era of demonstrating early-stage fault tolerance, requiring many qubits [1]. In this context, large-scale quantum computer simulation using classical computers has become more important than ever for finding potential applications or examining quantum systems without the need to construct and operate actual machines. Herein, the computational complexity is the bottleneck, which exponentially increases with the number of qubits [2].

The Tensor Network (TN) method, developed for solving many-body spin problems in statistical mechanics [3–6], has gained attention in various large-scale problems. The TN can significantly reduce the elements with low-rank approximation [7–9], typically with the decomposition of large-scale elements. A state vector describing a quantum state can be decomposed into a Matrix Product State (MPS) format with a Canonical Form (CF) for updating tensors [10–12]. MPS with CF is useful for one-dimensional quantum many-body spin problems interacting with only neighboring qubits each other. On the other hand, general quantum circuit with connections between distant qubits [13–15] make its simulation inefficient due to complexity to create CF.

This work proposes and evaluates several methods for simplifying the tensor updates compared with CF for MPS-based efficient quantum computer simulation. The methods examined include Simple Update (SU) method [16], which potentially shows a good performance-complexity tradeoff.

The rest of the paper is organized as follows. Sec. II summarizes the conventional TN methods with tensor updates based on CF. Sec. III shows tensor updates simplification methods including SU and those are numerically evaluated in Sec. IV. Sec. V concludes the work.

II. CONVENTIONAL METHODS

In this section, we review the conventional TN methods useful for the quantum computer simulation. We start from the approximation the State Vector (SV) with one of the simplest TN descriptions of Matrix Product

State (MPS). We then move to the methods for tensors updates in MPS and further specified that with. CF to orthogonalize the state [10], with starting the problem in applying CF to the quantum computer simulation.

A. Approximation with MPS

This work focuses on behaviors of qubits in quantum computers. The state of N qubits in quantum computers can be described with the SV as

$$|\psi\rangle = \sum_{\sigma_1 \sigma_2 \dots \sigma_N} C^{\sigma_1 \sigma_2 \dots \sigma_N} |\sigma_1\rangle |\sigma_2\rangle \dots |\sigma_N\rangle, \quad (1)$$

where $|\psi\rangle$, $C^{\sigma_1 \sigma_2 \dots \sigma_N}$, and $\sigma_i \in \{0, 1\}$ denote the state of N qubits in quantum computers, SV, and the physical index for the state of i -th qubit [17], respectively. It is difficult to exactly obtain the SV $C^{\sigma_1 \sigma_2 \dots \sigma_N}$ due to the numerous (2^N) elements in a tensor having N indices and, a degree of freedom of 2 in each index.

To reduce the number of elements, we employ MPS as shown in FIG. 1 to approximate the tensor $C^{\sigma_1 \sigma_2 \dots \sigma_N}$ using a set of rank-3 local tensors $\{M^{\sigma_i}\}$. The approximation of SV by MPS is expressed as

$$C^{\sigma_1 \sigma_2 \dots \sigma_N} \approx M^{\sigma_1} M^{\sigma_2} \dots M^{\sigma_N}, \quad (2)$$

where M^{σ_i} denotes a local tensor [10]. We also express the local tensor M^{σ_i} with virtual indices a_i, a_{i+1} explicitly as $M_{a_i, a_{i+1}}^{\sigma_i}$. We apply this notation to other tensors as well. The tensor multiplication follows a contraction rule,

$$M^{\sigma_{i-1}} M^{\sigma_i} = \left\{ \sum_{a_i}^D m_{a_{i-1}, a_i}^{\sigma_{i-1}} m_{a_i, a_{i+1}}^{\sigma_i} \right\}, \quad (3)$$

where D denotes a degree of freedom.

Each local tensor M^{σ_i} has $O(1)$ elements, enabling the simulation of quantum computers with a reduced number of elements. Unless otherwise stated, we use MPS throughout this paper.



FIG. 1. Tensor network diagrams of (a) SV and (b) MPS, where the nodes and the lines represent tensors and indices, respectively. The connected lines indicate a contraction. In this example, SV is represented by one rank-5 tensor, while the MPS consists of three rank-3 tensors and two rank-2 tensors.

B. Tensors updates in MPS

Both of qubit states and MPS's local tensors are updated by quantum gates, which are described with tensors, and are applied through tensor contraction [17]. According to [18], quantum gates can be decomposed into the elemental gates including one-qubit gates and two-qubit gates. We employ this tensor description with these elemental gates to update the tensors in MPS. Here, we explain the processes of applying one-qubit gates, adjacent two-qubit gates, and non-adjacent two-qubit gates, respectively.

One-qubit gate An one-qubit gate operation is described with the contraction of a local tensor $M_{a_i, a_{i+1}}^{\sigma_i}$ with a matrix $G^{\sigma'_i \sigma_i}$ representing the quantum gate [10], i.e.,

$$M_{a_{i-1}, a_i}^{\sigma_i} \rightarrow M'_{a_{i-1}, a_i}{}^{\sigma_i} = \sum_{\sigma'_i} M_{a_{i-1}, a_i}^{\sigma'_i} G^{\sigma'_i \sigma_i}. \quad (4)$$

After this one-qubit gate operation, $M'_{a_i, a_{i+1}}{}^{\sigma_i}$ becomes the new local tensor.

Adjacent two-qubit gate A two-qubit gate operation is expressed by a rank-4 tensor [19]. An adjacent two-qubit gate is denoted as

$$\begin{aligned} & \sum_{a_i} M_{a_{i-1}, a_i}^{\sigma_i} M_{a_i, a_{i+1}}^{\sigma_{i+1}} \\ & \rightarrow \sum_{\sigma'_i, \sigma'_{i+1}, a_i} M_{a_{i-1}, a_i}^{\sigma'_i} M_{a_i, a_{i+1}}^{\sigma'_{i+1}} G^{\sigma'_i \sigma_i \sigma'_{i+1} \sigma_{i+1}} = T_{a_{i-1}, a_{i+1}}^{\sigma_i \sigma_{i+1}}, \end{aligned} \quad (5)$$

where $G^{\sigma'_i \sigma_i \sigma'_{i+1} \sigma_{i+1}}$ is a rank-4 tensor representing adjacent two-qubit gate, and $T_{a_{i-1}, a_{i+1}}^{\sigma_i \sigma_{i+1}}$ is the rank-4 tensor contracted by the summation over σ'_i , σ'_{i+1} , and a_i . To maintain the network topology before and after the gate operation, the obtained rank-4 tensor is decomposed into two rank-3 tensors $\sum_{a_i}^{D'} M_{a_{i-1}, a_i}^{\sigma_i} M_{a_i, a_{i+1}}^{\sigma_{i+1}}$. The degree of freedom is changed from D to D' during the process. Here, D' is truncated under certain conditions, e.g., D exceeds the threshold, a new D is generated. This approximation is known as a low-rank approximation [20], realized by Singular Value Decomposition (SVD) in this work.

Non-adjacent two-qubit gate We apply non-adjacent (i -th and j -th) two-qubit gates. We discuss the process of applying non-adjacent two-qubit gates between the i -th qubit and the j -th qubit. We apply non-adjacent two-qubit gates by swapping the physical indices, σ_i and σ_{i+1} , as

$$\begin{aligned} & \sum_{a_i}^D M_{a_{i-1}, a_i}^{\sigma_i} M_{a_i, a_{i+1}}^{\sigma_{i+1}} \\ & \approx \sum_{a_i=1}^D \tilde{M}_{a_{i-1}, a_i}^{\sigma_{i+1}} \tilde{M}_{a_i, a_{i+1}}^{\sigma_i}. \end{aligned} \quad (6)$$

This process includes the following steps [21]:

STEP1: Contract two local tensors, $M_{a_{i-1}, a_i}^{\sigma_i}$ and $M_{a_i, a_{i+1}}^{\sigma_{i+1}}$ into a rank-4 tensor $T_{a_{i-1}, a_{i+1}}^{\sigma_i, \sigma_{i+1}}$.
STEP2: Reshape the tensor $T_{a_{i-1}, a_{i+1}}^{\sigma_i, \sigma_{i+1}}$ into a matrix $\tilde{T}_{a_{i-1}, \sigma_{i+1}}^{a_{i+1}, \sigma_i}$.
STEP3: Decompose the matrix $\tilde{T}_{a_{i-1}, \sigma_{i+1}}^{a_{i+1}, \sigma_i}$ into $\sum_{k=1}^{D'} A_{a_{i-1}, k}^{\sigma_{i+1}} S_{k, k} B_{a_{i+1}}^{\sigma_i}$ using SVD, where $S_{k, k}$ is the matrix composed of singular values and $A_{a_{i-1}, k}^{\sigma_{i+1}}$ and $B_{a_{i+1}}^{\sigma_i}$ are the tensor reshaped from unitary matrices in SVD. The local tensor with σ_i is moved by swapping physical indices in Eq. (6) repeatedly until being adjacent to the local tensors with σ_j . After the adjacent two-qubit gate in Eq. (5), swapping physical indices in Eq. (6) is again repeatedly applied to maintain the index order before and after the operation.

C. Canonical form

The MPS format can further be approximated by low-rank approximation, which truncates some vectors based on tensors decomposition. CF is a description of decomposed tensors [10] and influence the performance of the approximation. The qubit state in Eq. (1) is described with the Schmidt decomposition

$$|\psi\rangle = \sum_k S_{k, k} |x_k\rangle_X |y_k\rangle_Y, \quad (7)$$

given by SVD of SV $C^{\sigma_1 \sigma_2 \dots \sigma_N} = \sum_k U_{\sigma_1 \sigma_2 \dots \sigma_m, k} S_{k, k} V_{\sigma_{m+1} \dots \sigma_N, k}^*$ with the decomposition subsystems X and Y , Schmidt bases $x_k = U_{\sigma_1 \sigma_2 \dots \sigma_m, k} |\sigma_1\rangle |\sigma_2\rangle \dots |\sigma_m\rangle$, and $y_k = \sum_{\sigma_{m+1} \dots \sigma_N} V_{\sigma_{m+1} \dots \sigma_N, k}^* |\sigma_{m+1}\rangle \dots |\sigma_N\rangle$, and Schmidt coefficients $S_{k, k}$ [10]. Here, singular values and unitary matrices in SVD corresponds to Schmidt coefficients and basis transformation, respectively. Truncating, i.e., ignoring the Schmidt coefficients except for ones having D largest values and related Schmidt bases, in Eq. (7) is can minimize the error with the low-rank approximation of SV under a given D .

To avoid the complexity in the Schmidt decomposition in Eq. (7) due to the exponentially large degrees of freedom x_k and y_k , CF of MPS represented as

$$C^\sigma = A^{\sigma_1} \dots A^{\sigma_m} \Lambda B^{\sigma_{m+1}} \dots B^{\sigma_N} \quad (8)$$

where σ denotes $\{\sigma_1\sigma_2\dots\sigma_N\}$, A^{σ_i} and B^{σ_i} are normalized as $\sum_{\sigma_i} A^{\sigma_i\dagger} A^{\sigma_i} = I$, $\sum_{\sigma_i} B^{\sigma_i} B^{\sigma_i\dagger} = I$, respectively, m denotes the position of the Schmidt coefficients, and Λ is the diagonal matrix [10]. In CF, the local matrices with a physical index in subsystem X are transformed into left normalized matrices $\{A^{\sigma_i}\}$ and those in subsystem Y are transformed into right normalized matrices $\{B^{\sigma_i}\}$. CF in Eq. (8) is obtained from the iterative operations of the QR decomposition $M^{\sigma_i} = A^{\sigma_i}R$ and the contraction $RM^{\sigma_{i+1}} = \tilde{M}^{\sigma_{i+1}}$, where R is the upper triangular matrix given by the QR decomposition from M^{σ_i} . CF of MPS corresponds to Schmidt decomposition [22], i.e., $(A^{\sigma_1}\dots A^{\sigma_m})$, $(B^{\sigma_{m+1}}\dots B^{\sigma_N})$ and Λ correspond to Schmidt bases (x_k , and y_k) and Schmidt coefficients $S_{k,k}$, respectively. Note that, this paper employs S as singular values of arbitrary matrix regardless whether these are Schmidt coefficients, while Λ as Schmidt coefficients. Singular values of SV or a matrix in CF are described with either S or Λ , while singular values of other matrices are only denoted by S . As well as the truncation in the Schmidt decomposition, the truncation in CF is useful because of the performance under a given dimension.

D. Problems of CF-based quantum computing simulation

Quantum computing generally requires two-qubit gates between arbitrary (adjacent or distant) qubit pairs. To simulate distant two-qubit gates, the position of the Schmidt coefficients m in Eq. (8) should be changed to swap the physical indices as shown in Sec. II B. Thus, the complexity increases depending on the qubit distance in the quantum gate and the position change among the consecutive time step.

In order to address the problems above, we introduce simplified tensor update methods for efficient quantum computing simulation with arbitrary quantum gates in Sec. III, and their performance-complexity tradeoff is numerically analyzed in Sec. IV.

III. PROPOSED METHODS

MPS-based quantum computer simulation usually employs CF, leading to high complexity in tensor updates reviewed in the previous section. This section proposes the tensor updates simplification methods by discarding some singular values.

CF is usually understood in the context of Schmidt decomposition [22]. On the other hand, it is also regarded as a form that all singular values among local tensors are collected into a matrix Λ , representing Schmidt coefficients.

We expect that the dominance of singular values can vary depending on the target system and subsystems X and Y . Singular values far from the area of subsystem X and Y are expected to be ignorable. This idea is similar

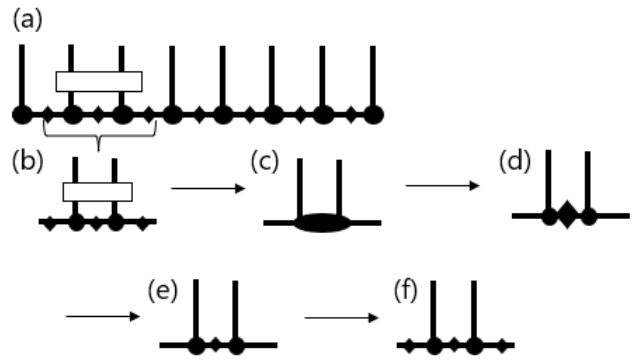


FIG. 2. The procedure of SU: (a) ansatz of the SU, (b) tensors around quantum gate, (c) tensor after contraction, (d) decomposed tensors, (e) approximated tensors, and (f) reverted form of tensors.

to the approximation of MPS, which disregards entanglements between distant local tensors. Our proposal thus includes selectively absorbing singular values.

A. Simple update

Our main proposal for the tensor updates simplification is based on SU, which is originated in simulating high-dimensional quantum many-body spin systems [16]. FIG. 2 shows the SU procedure customized to MPS. Adjacent two-qubit gate operation with SU consists of the following steps:

(a) Use an ansatz which diagonal matrices S^j ($j = 1, \dots, N-1$) between local tensors having a physical index $M^{\sigma_1} S^1 M^{\sigma_2} \dots S^{N-1} M^{\sigma_N}$ with the quantum gate $G^{\sigma'_i \sigma_i \sigma'_{i+1} \sigma_{i+1}}$.

(b) Select tensors around quantum gate from MPS as $\sum_{\sigma', k} S_{a_{i-1}, k_{i-1}}^{i-1} M_{k_{i-1}, k_i}^{\sigma'_i} S_{k_i, k_i}^i M_{k_i, k_{i+1}}^{\sigma_{i+1}} S_{k_{i+1}, a_{i+1}}^{i+1} G^{\sigma'_i \sigma_i \sigma'_{i+1} \sigma_{i+1}}$.

(c) Contract selected tensors as $M_{a_{i-1}, a_{i+1}}^{\sigma_i, \sigma_{i+1}}$.

(d) Decompose the contracted tensors by SVD as $\sum_{a_i}^{D'} U_{a_{i-1}, a_i}^{\sigma_i} S_{a_i, a_i} V_{a_i, a_{i+1}}^{\dagger \sigma_{i+1}}$, where $D' = \min(2 \times D_{a_{i-1}}, 2 \times D_{a_{i+1}})$.

(e) Approximate the diagonal matrix made by SVD as $\sum_{a_i}^D U_{a_{i-1}, a_i}^{\sigma_i} S_{a_i, a_i} V_{a_i, a_{i+1}}^{\dagger \sigma_{i+1}}$, where $D = \min(2 \times D_{a_{i-1}}, 2 \times D_{a_{i+1}}, D_{\max})$ and D_{\max} is a hyperparameter.

(f) Revert contracted adjacent diagonal tensors as $\sum S_{a_{i-1}, a_{i-1}}^{i-1} M'_{a_{i-1}, a_i}^{\sigma'_i} S'_{a_i, a_i} M'_{a_i, a_{i+1}}^{\sigma_{i+1}} S_{a_{i+1}, a_{i+1}}^{i+1}$.

A non-adjacent two-qubit gate operation is executed with iteration of swap gates, and the process of the SU also includes the steps explained above. SU utilizes adjacent singular values only thus can reduce the complexity compared with deriving CF.

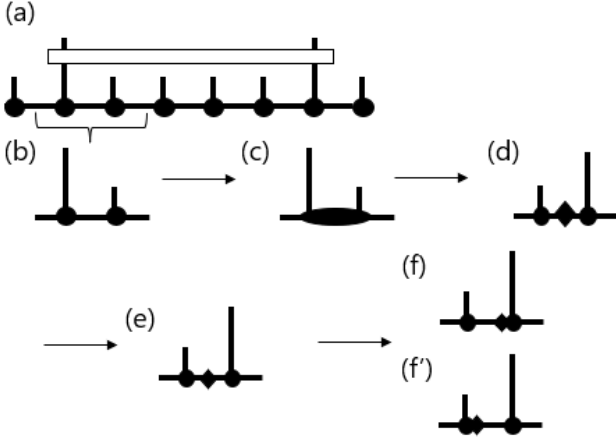


FIG. 3. The procedures for the two low-complexity alternatives in our study: (a) ansatz of alternatives, (b) two tensors targeted for swapping, (c) tensor after contraction, (d) decomposed tensors, (e) approximated tensors, (f) reverted form of tensors in the PCF method, and (f') reverted form of tensors in the NF method. The moved tensor iteratively absorbs the diagonal matrix during the series of the swap processes in (f), unlike in (f'). The extended line segments in this figure represent the physical indices where a non-adjacent two-qubit gate is applied.

B. Low-complexity alternatives

This work compares SU with other alternatives depicted in FIG. 3. They treat singular values in different manners so that the number of absorbing singular values of each update is limited to less than proportional to the number of qubits N . FIG. 3 exemplified quantum gates for two distant i -th (left) and j -th (right) qubits, requiring swaps of, e.g., i -th quantum gates repeatedly after updating the target tensor. We compare the fidelity of the three methods in Sec. IV, the first evaluation.

Partial canonical form. Singular values are absorbed with the movement of target tensors with a swap based on Eq. (6), i.e.,

$$\begin{aligned} & \sum_{\{a_i | i \in \{1, \dots, N-1\}\}} M_{a_1}^{\sigma_1} \dots M_{a_i, a_{i+1}}^{\sigma_i} M_{a_{i+1}, a_{i+2}}^{\sigma_{i+1}} \dots M_{a_{N-1}}^{\sigma_N} \\ & \approx \sum_{\{a_i\}} M_{a_1}^{\sigma_1} \dots A_{a_i, a_{i+1}}^{\sigma_{i+1}} \left(\sum_k S_{a_{i+1}, k} M_{k, a_{i+2}}^{\sigma_i} \right) \dots M_{a_{N-1}}^{\sigma_N}. \end{aligned} \quad (9)$$

similar to many-body spin systems. This process repeats until the local tensors with σ_i and those with σ_j become

adjacent, whose quantum state is given by

$$\begin{aligned} & \sum_{\{a_i\}} M_{a_1}^{\sigma_1} \dots M_{a_{i-2}, a_{i-1}}^{\sigma_{i-1}} A_{a_{i-1}, a_i}^{\sigma_{i+1}} \dots A_{a_{j-3}, a_{j-2}}^{\sigma_{j-1}} \\ & A_{a_{j-2}, a_{j-1}}^{\sigma_i} \left(\sum_k S_{a_{j-1}, k} M_{k, a_j}^{\sigma_j} \right) M_{a_j, a_{j+1}}^{\sigma_{j+1}} \dots M_{a_{N-1}}^{\sigma_N}. \end{aligned} \quad (10)$$

A quantum gate $G^{\sigma'_i, \sigma_i, \sigma'_{i+1}, \sigma_{i+1}}$ is applied to the state in Eq. (10) and a low-rank approximation is performed. After that, to revert the physical index σ_i back to its original site, the steps of Eq. (10) are followed in reverse order, i.e.,

$$\begin{aligned} & \sum_{\{a_i\}} M_{a_1}^{\sigma_1} \dots M_{a_{i-2}, a_{i-1}}^{\sigma_{i-1}} \left(\sum_k A_{a_{i-1}, k}^{\sigma_i} S_{k, a_i} \right) \\ & B_{a_i, a_{i+1}}^{\sigma_{i+1}} \dots B_{a_{j-1}, a_j}^{\sigma_j} M_{a_j, a_{j+1}}^{\sigma_{j+1}} \dots M_{a_{N-1}}^{\sigma_N}. \end{aligned} \quad (11)$$

We call this method Partial Canonical Form (PCF) because the tensors between i -th and j -th positions are similar to Eq. (8). PCF takes singular values between qubits with non-adjacent two-qubit gate operation into account.

Non-normalized form. Singular values of moved tensors are not absorbed, i.e.,

$$\begin{aligned} & \sum_{\{a_i\}} M_{a_1}^{\sigma_1} \dots M_{a_i, a_{i+1}}^{\sigma_i} M_{a_{i+1}, a_{i+2}}^{\sigma_{i+1}} \dots M_{a_j, a_{j+1}}^{\sigma_j} \dots M_{a_{N-1}}^{\sigma_N} \\ & \approx \sum_{\{a_i\}} M_{a_1}^{\sigma_1} \dots \left(\sum_k A_{a_i, k}^{\sigma_{i+1}} S_{k, a_{i+1}} \right) M_{a_{i+1}, a_{i+2}}^{\sigma_i} \\ & \dots M_{a_j, a_{j+1}}^{\sigma_j} \dots M_{a_{N-1}}^{\sigma_N}. \end{aligned} \quad (12)$$

The remaining processes of this method are identical to PCF. The normalized tensor $A^{\sigma_{i+1}}$ is contracted with a diagonal matrix S , resulting in non-normalized tensors prior to the next swap. We call this method Non-normalized Form (NF).

IV. EVALUATION

This section numerically evaluates the simplified tensor update methods proposed in Sec. III, which absorb singular values in different manners. First, we compare their fidelities on randomly adjacent or distant quantum gates with 20 qubits and discuss the results from the viewpoint of singular values. Second, we further examine the best one in terms of both fidelity and complexity on randomly adjacent quantum gates until 1000 qubits.

A. Fidelity

The approximation performance in MPS-based quantum computing simulation is quantified by fidelity referred to SV. Higher fidelity would be obtained from the

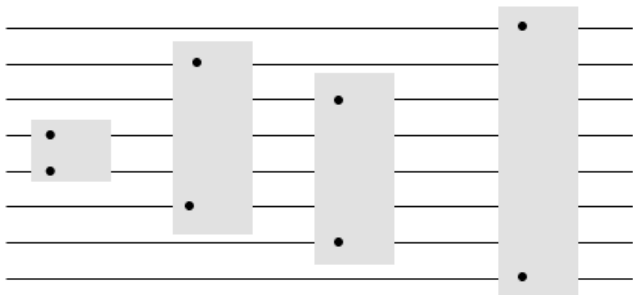


FIG. 4. A portion of exemplified quantum circuit for fidelity analysis. This kind of circuitry is employed for the quantum volume measurement. Circles represent qubits for the quantum gate operation.

method extracting more dominant singular values. SU ignores singular values far from the target gates. Distant singular values are expected to be trivial because the entanglement between distant qubits is less significant in the MPS approximation [23]. Thus, it can be anticipated that the fidelity of SU shows a higher value than the other alternatives.

Numerically simulation conditions are explained. FIG. 4 shows a portion of quantum circuit to compare the fidelities among proposed methods and conventional CF. This kind of circuitry is usually used to measure the quantum volume, which can be decomposed into elemental quantum gates operated over one or two qubits. For setting up the quantum circuit, *Qiskit* library was employed, FIG. 4 focuses on the area with the number of qubits of 8 and the depth of 1, where the depth refers to the layers of SU(4) operations in the quantum circuit [24]. A two-qubit gate is applied to a random pair of qubits, resulting in the entanglement of those. This test case is intended to compare the tensor update methods having different singular values absorption feature, although the case including distant entanglement is difficult to approximate for MPS even with the tensor updates by CF and proposed methods. There are several truncation parameters as follows: the number of effective singular values ≤ 40 , each effective absolute singular value ≥ 0.01 , and the effective singular value to largest singular value ratio $\geq 1\%$. The number of qubits N was 20. Note that the random quantum circuit generated by *Qiskit* was 30 times repeatedly examined, whose seed was given by a pseudorandom number generator. Here, the performance metric is the fidelity

$$F_{\text{SV}} = |\langle \psi_{\text{SV}} | \psi_{\text{TN}} \rangle|^2, \quad (13)$$

between the qubit states obtained by SV ($|\psi_{\text{SV}}\rangle$) and that by TN ($|\psi_{\text{TN}}\rangle$) including conventional CF and the proposed three simplification methods. When the state obtained by TN method equals that by SV, $F_{\text{SV}} = 1$. FIG. 5 shows the average and standard deviation of the obtained fidelities. Due to the difficult condition to MPS,

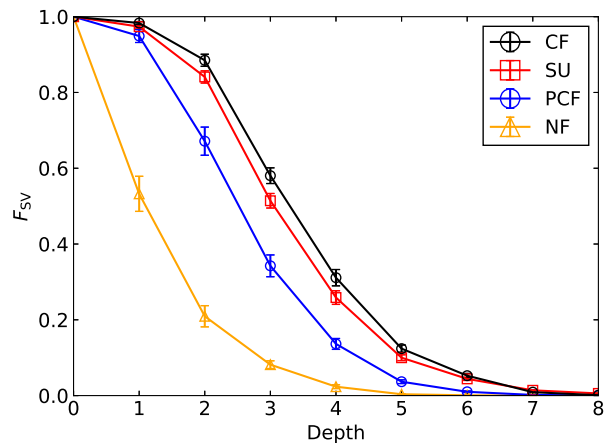


FIG. 5. Numerically simulated fidelities F_{SV} for CF and the three proposed methods.

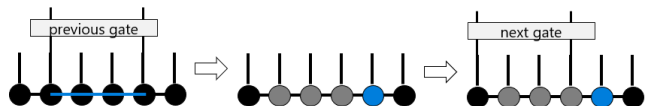


FIG. 6. Concept of singular value absorption in the proposed methods. PCF does not absorb singular values during the switching of quantum gates and leave the singular values there.

the fidelity rapidly decreases as increasing the depth, even with CF. Among the proposed methods, SU and NF show the highest and lowest fidelities, respectively. In the following discussion, the fact that the fidelity of SU close to CF means that SU could absorb important singular values in this examination. Fidelities of PCF is comparably high for the depth of 1 but significantly low for larger depths. It is because that PCF moves singular values but, does not absorb them in swapping the quantum gates as shown in FIG. 6, while SU always absorbs singular values of adjacent qubits.

B. Computational cost

The approximation is expected to reduce the complexity. Here we evaluation the computational cost. According to the first evaluation results that SU is suitable for tensor updates simplification, only SU and CF are compared with an MPS-suitable quantum computer simulation case. In the complexity evaluation, we employ a quantum circuit with adjacent random quantum gates as shown in FIG. 7. The quantum gates order is randomly chosen and the quantum gates allocation can be nonuniform. Some qubits can have more quantum gates operation than the others. We execute multiple iterations by changing the seed of the pseudorandom number

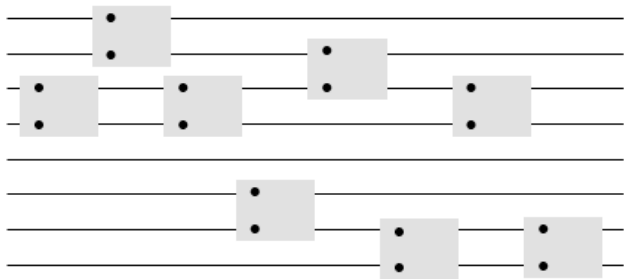


FIG. 7. A portion of exemplified quantum circuit with adjacent random quantum gates. Though this figure includes only 8 qubits for a small example, we evaluated up to 1000 qubits.

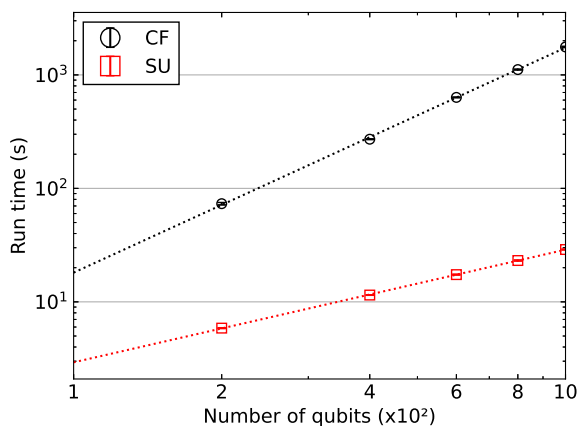


FIG. 8. Run time in tensor updates through numerical simulation. Dotted lines are regression lines. SU significantly reduce the run time for a large number of qubits N . Log-scale slopes are around 2 for CF and 1 for SU, respectively.

generator. While there are methods to reduce computational cost by optimizing the order of the quantum gates [25, 26], it would be a challenging issue [27]. This evaluation excludes, the optimization of the quantum gates order. Regarding the truncation parameters, the number of effective singular values ≤ 10 . The number of random quantum circuits generation was 5 times. The number of qubits N was variable that of quantum gates was the same as N . The other parameters are the same as those in the first evaluation. In this setup, we quantify the computation run time as a complexity metric and fidelity referenced to CF,

$$F_{CF} = |\langle \psi_{CF} | \psi_{SU} \rangle|^2, \quad (14)$$

where $|\psi_{CF}\rangle$ and $|\psi_{SU}\rangle$ denotes the qubit states given by CF and SU, respectively. FIG. 8 shows the run time for tensor updates. The SU significantly reduced the run time in cases of a large number of qubits N , e.g., SU shows 61 times shorter than CF for $N = 1000$. In

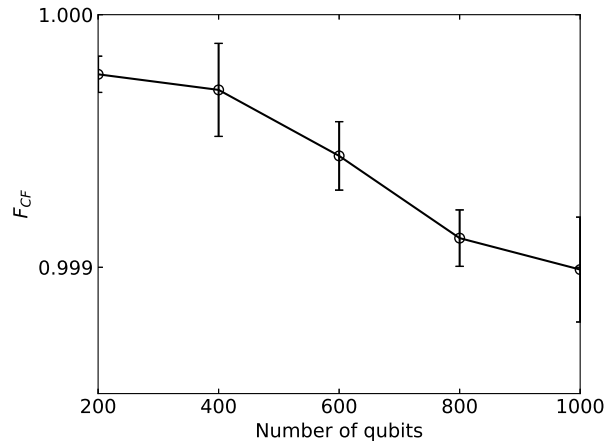


FIG. 9. Numerically obtained fidelity F_{CF} (defined in Eq. (14)). Qubits states given by CF and SU are almost identical.

a log scale view, the slope of the run time against N is approximately 2 for CF and 1 for SU, respectively. Roughly saying, the run time is proportional to N^2 for CF and proportional to N , thus SU reduces the computational costs by $O(N)$. CF consumes significant complexity as explained in Sec. IID, and SU can skip it. The average distance between two time-consecutive quantum gates in a qubit is $O(N)$ for randomly ordered quantum gates, which requires the change of position (m in Eq.(8)) at $O(N)$ complexity. CF requires the $O(N)$ complexity given by QR decomposition and absorbing the matrix R , but SU does not. FIG. 9 shows the fidelity F_{CF} in Eq. (14). The fidelity is higher than 0.998, i.e., the qubit states given by CF and SU are almost the same. According to these results, SU shows a good balance of performance (fidelity) and complexity (computational cost, i.e., run time) in MPS-based quantum computing simulation.

V. CONCLUSION

We worked on the simplification of MPS-based quantum computer simulation, especially we focused on its tensor updates methods. There are two aspects to be considered, i.e., performance (fidelity) and complexity (computational cost). In terms of the network architecture, compared with the reference of SV, MPS approximates qubits state. Regarding the tensor updates, the reference of CF absorbs all singular values in MPS, which causes a high complexity. Thus we simplified it by ignoring some singular values. Our proposal for the tensor updates includes SU, absorbing adjacent singular values, which can dominate MPS-based quantum computer simulation. Obtained results of fidelities and computational cost (run time) agree well with our original thoughts, i.e., the qubits states given by SU were almost

the same as that by CF. Through the simulation of random operations limited to adjacent quantum gates, which is suitable to MPS, SU reduced the run time by $O(N)$ compared with CF at almost identical fidelities. More quantitatively, SU shortened the run time by around 61 times against CF at fidelities around 0.999 in quantum circuit having 1000 qubits and 1000 adjacent two-qubit gates.

Acknowledgments

We would like to express our gratitude to Shota Koshikawa, Isamu Kudo, Alifu Xiafukaiti, and Narumitsu Ikeda of Mitsubishi Electric Corp. for fruitful discussions. We also wish to extend our thanks to George Monma, Tatsuo Kaniwa, Gaku Nagashima, and Yuichiro Minato from blueqat Inc. for providing the research environment and technical support.

-
- [1] D. Bluvstein, S. J. Evered, A. A. Geim, S. H. Li, H. Zhou, T. Manovitz, S. Ebadi, M. Cain, M. Kalinowski, D. Hangleiter, et al., *Nature* **626**, 58 (2024).
 - [2] Z. Wang, Z. Chen, S. Wang, W. Li, Y. Gu, G. Guo, and Z. Wei, *Scientific Reports* **11**, 355 (2021).
 - [3] S.R.White, *Phys.Rev.Let* **69**, 2863 (1992).
 - [4] S.Ostlund and S.Rommer, *Phys.Rev.Let* **75**, 19 (1995).
 - [5] M.-D. M.Roncaglia and G.Sierra, *Phys. Rev. B* **64**, 075117 (2004).
 - [6] F.Verstraete and J.I.Cirac, arXiv:cond-mat p. 0407066 (2004).
 - [7] Y.A.Liu, X.L.Liu, F.N.Li, H.Fu, Y.Yang, J.Song, P.Zhao, Z.Wang, D.Peng, H.Chen, et al., SC '21: Proceedings of the International Conference for High Performance Computing, Networking, Storage and Analysis pp. 1–12 (2021).
 - [8] J. Tindall, M. Fishman, E. M. Stoudenmire, and D. Sels, *PRX Quantum* **5**, 010308 (2024).
 - [9] E. C. Martín, K. Plekhanov, and M. Lubasch, *Quantum* **7**, 974 (2023).
 - [10] U. Schollwoeck, *Annals of Physics* **326**, 96 (2011).
 - [11] H. N. Phien, G. Vidal, and I. P. McCulloch, *Phys. Rev. B* **86**, 245107 (2012).
 - [12] A. McCaskey, E. Dumitrescu, M. Chen, D. Lyakh, and T. Humble, *PLOS ONE* (2018).
 - [13] Y. Wu, W. Bao, S. Cao, F. Chen, M. Chen, X. Chen, T. Chung, H. Deng, Y. Du, D. Fan, et al., *Phys. Rev. Lett.* **127**, 180501 (2021).
 - [14] S. Boixo, S. V. Isakov, V. N. Smelyanskiy, R. Babbush, N. Ding, Z. Jiang, M. J. Bremner, J. M. Martinis, and H. Neven, *Nature Physics* **14**, 595 (2018).
 - [15] Q. Zhu, S. Cao, F. Chen, M. Chen, X. Chen, T. Chung, H. Deng, Y. Du, D. Fan, M. Gong, et al., *Science Bulletin* **67**, 240 (2022).
 - [16] H. C. Jiang, Z. Y. Weng, and T. Xiang, *Phys.Rev.Let* **101** p. 090603 (2008).
 - [17] J. Biamonte and V. Bergholm, arXiv (2017), 1708.00006.
 - [18] A. Barenco, C. H. Bennett, R. Cleve, D. P. DiVincenzo, N. Margolus, P. Shor, T. Sleator, J. A. Smolin, and H. Weinfurter, *Phys. Rev. A* **52**, 3457 (1995).
 - [19] F. Vatan and C. Williams, *Phys. Rev. A* **69**, 032315 (2004).
 - [20] N. K. Kumar and J. Shneider, arXiv preprint arXiv:1606.06511 (2016).
 - [21] NVIDIA, *cuquantum: Mps algorithms*, https://github.com/NVIDIA/cuQuantum/blob/main/python/samples/cutensornet/tn_algorithms/mps_algorithms.ipynb (2021), accessed: May 8th 2024, Branch: main.
 - [22] H. A.Higuchi and A.Sudbery, arXiv:quant-ph p. 0006125 (2002).
 - [23] I. Cirac, D. Perez-Garcia, N. Schuch, and F. Verstraete, *Rev. Mod. Phys.* **93**, 045003 (2021).
 - [24] *Qiskit: An open-source framework for quantum computing. quantum volume.*, <https://docs.quantum.ibm.com/api/qiskit/qiskit.circuit.library.QuantumVolume> (2024).
 - [25] C. Huang, F. Zhang, M. Newman, X. Ni, D. Ding, J. Cai, X. Gao, T. Wang, F. Wu, G. Zhang, et al., *Nature Computational Science* **1**, 578–587 (2021).
 - [26] Y. Akhremtsev, T. Heuer, P. Sanders, and S. Schlag, in *2017 Proceedings of the Nineteenth Workshop on Algorithm Engineering and Experiments (ALENEX)* (2017), pp. 28 – 42.
 - [27] E. A. Meiroum, H. Maron, S. Mannor, and G. Chechik, arXiv:2204.09052 [quant-ph] (2022).